Civil Engineering Applications: Specific Properties of NiTi Thick Wires and Their Damping Capabilities, A Review

Vicenç Torra, Ferran Martorell, Francisco C. Lovey & Marcos Leonel Sade

Shape Memory and Superelasticity
Advances in Science and Technology

ISSN 2199-384X

Shap. Mem. Superelasticity
DOI 10.1007/s40830-017-0135-y

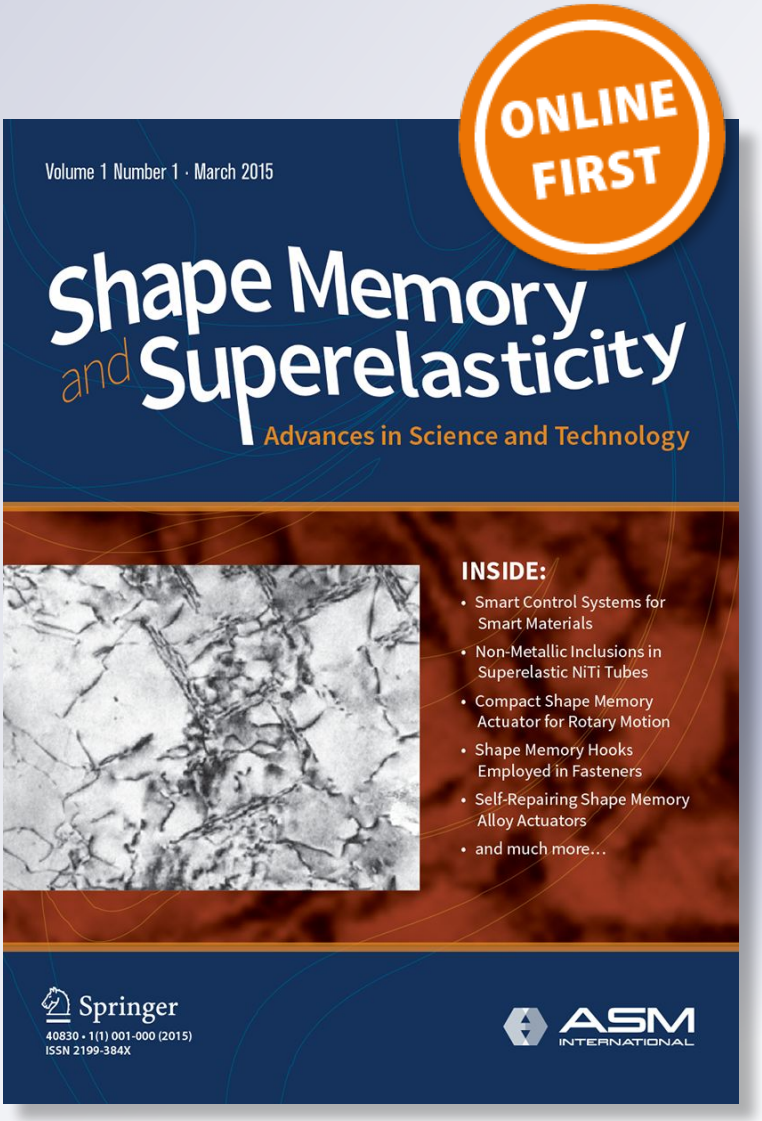

Springer

Shap. Mem. Superelasticity
https://doi.org/10.1007/s40830-017-0135-y

Civil Engineering Applications: Specific Properties of NiTi Thick Wires and Their Damping Capabilities, A Review

Vicenç Torra[1] · Ferran Martorell[2] · Francisco C. Lovey[3] · Marcos Leonel Sade[3]

Abstract This study describes two investigations: first, the applicability of NiTi wires in the damping of oscillations induced by wind, rain, or traffic in cable-stayed bridges; and second, the characteristic properties of NiTi, i.e., the effects of wire diameter and particularly the effects of summer and winter temperatures and strain-aging actions on the hysteretic behavior. NiTi wires are mainly of interest because of their high number of available working cycles, reliable results, long service lifetime, and ease in obtaining sets of similar wires from the manufacturer.

Keywords Shape memory alloys · NiTi alloy · Damping in stayed cables · Wire improvements · Summer–winter effects · Strain aging

Introduction

Many physical systems exhibit *phase transitions*, characterized by singularities in a thermodynamic potential, such as the free energy, and hence by discontinuities in the derivative of that potential. The pioneering work of P. Ehrenfest published in 1933 [1] classified phase transitions according to the ordinal number (first, second, etc.) of the derivative of the free energy that showed the discontinuity; these were called first-order, second-order, etc., transitions, respectively. Because the first derivative of the relevant thermodynamic potential is discontinuous for a first-order phase transition, such a transition is usually accompanied by a latent heat. Currently, both discontinuities and divergences at the phase-transition point are understood as important. All higher-order phase transitions are grouped as either *critical*- or *continuous*-phase transitions; the term "continuous" as applied to phase transitions was introduced by Landau in his classic paper on the theory of phase transitions [2].

The martensitic transformation (MT) is the origin of the particular properties of shape memory alloys (SMAs). The MT is considered a solid–solid first-order phase transition with hysteresis between metastable phases. SMAs are smart materials with many practical and potential applications. Several applications are health solutions, such as using SMAs in orthodontic applications; they have also been studied for use in dampers in civil engineering and for their actions in morphing. Experimental analysis of SMAs shows hysteretic behaviors in stress–strain or strain–temperature representations. In fact, representations of multiple continuous stress–strain cycles show monotonic SMA creep and the practical reduction of the available deformation associated with the cross sections of the samples. In temperature-induced transformations without external stresses, interactions between martensite variants can extend the transformation temperatures by more than 30 K. These interactions significantly increase the difference between M_s (martensite start) and M_f (martensite finish). The asymptotic increase of creep in stress-induced transformations and the larger differences between M_s and M_f suggest nonclassical phase-transition behavior in SMAs compared to conventional phase transitions over extremely small temperature spans. The SMA creep of wires is the

✉ Vicenç Torra
vtorra_1@yahoo.com

[1] Polytechnical University of Catalonia - Applied Physics (Retired), 08034 Barcelona, Catalonia, Spain

[2] PRG, Villarroel 162, 08036 Barcelona, Catalonia, Spain

[3] Centro Atomico de Bariloche, Instituto Balseiro and CONICET - Materials Physics, 8400 San Carlos de Bariloche, Rio Negro, Argentina

Published online: 04 December 2017

increase in length induced by repeated working cycles, i.e., an effect of fatigue on the material. The alloy composition and heat-treatment history determine the material's transformation behavior [3, 4].

In general, the MT is considered a first-order phase transition with an associated latent heat that, furthermore, required a constant stress in the transformation from the parent phase to martensite, accompanying changes in the transformation strain reaching up to 10%. In the late 1980s [3], the appearance of "minor actions" as the intrinsic thermoelasticity and its associated pseudoelasticity in single crystals of CuAlZn suggested difficulties in the classical analysis of SMAs. For instance, single-interface measurements suggested some minor difficulties with the classical idea of a first-order transformation in the SMA. Studies of the damping of SMAs realized by 2.46-mm diameter NiTi wires [5–10] established the appearance of S-shaped cycles, i.e., an inherent behavior unlike the flat cycles typical of thinner wires. The intrinsic S-slopes appear in stress–strain representations without thermal effects induced by cycling rate actions. At reduced cycling frequencies, the release and absorption of latent heat induce corresponding temperature increases and decreases. At high cycling frequencies, the hysteresis effect is more relevant, inducing only one net heating.

Interest in SMAs has increased for the last three decades because of their potential applications [11, 12]. This interest was recently further enhanced by the inclusion of standard courses on smart materials in the core engineering curricula at many universities worldwide. Thus far, SMAs have mainly been applied in health fields. The classic NiTi alloy [13, 14] is innocuous in the human body. Other newly developed Ti-based alloys have attracted interest because they show complete biological compatibility in practical situations. A focused axis of Ti-based alloys without Ni has been under continuous research by the Miyazaki group at the University of Tsukuba [15–18]. Several SMA applications are available commercially, including stents, surgical tools, orthodontic wires and bolts, and elements for bone and tooth reconstruction. The numbers of useful and efficient applications have also increased in other fields, such as automotive and consumer electronics, but these comprise a relatively small number of overall SMA uses. Several applications are detailed in the references [19–21].

This study synthesizes several experiments using NiTi wires and focuses on two general investigations. The first explores examples of oscillatory damping by SMA realized in cables in facilities using NiTi wires. The second one relates the comparative properties of thick and thin NiTi wires and characterizes the advantages of thick wires under the actions of external summer–winter temperatures. Furthermore, the eventual increase in maximal stress induced by strain aging is discussed.

Part One: Stayed Cables and Damping with SMAs

In recent years, the potential applicability of SMAs in damping devices for civil structures has attracted increasing interest. In particular, the smoothing of oscillations in buildings and bridges produced by earthquakes, winds, rain, traffic, and other natural phenomena is critical. The pseudoelastic effect and the hysteresis cycle associated with the MT in SMAs have been suggested to convert the mechanical energy of such oscillations into heat. Several authors [22–33] have researched damping in civil engineering using SMAs; the reviews of R. DesRoches (Atlanta, USA) and M. Dolce (Basilicata, Italy) describe these efforts [32, 33]. Re-centering is a significant problem in rubber and steel disk bearings used in seismically isolated buildings. The positive re-centering action of the pseudoelastic effect suggests different options, such as mixtures of martensitic and pseudoelastic bars for, respectively, damping versus damping and re-centering actions.

Coupled thermomechanical aspects include the critical stresses that induce pseudoelastic effects as a function of the working temperature through the Clausius–Clapeyron (CC) equation [9, 34–36]. In addition, latent heat is associated with the MT, which in turn depends on the applied transformation stress. Thus, the temperature of the specimen depends on the dissipation and absorption conditions of the latent heat during the transformation and retransformation, respectively. Among these conditions, parameters such as the deformation rate, dissipative media of the surroundings (for example, air convection), specimen size, and others all affect the temperature. Therefore, the CC equation affects the pseudoelastic behavior and the damping capacity in two ways. First, important changes in the specimen temperature are associated with either the self-heating phenomenon or changes in the working temperature. Two concomitant actions of changes of self-heating and external working temperatures therefore change the transformation stresses. Consequently, the stiffness and the resonance frequencies of structures with integrated SMA damping devices are dependent on the SMA temperature. Second, the shape of the hysteresis cycle and the hysteresis area itself also depend on the various aforementioned conditions. Because of the complexity of all these coupled phenomena, the real behaviors of the SMA elements must be experimentally tested following requirements for specific applications.

Recently, SMAs were studied as passive damping elements for civil structures utilizing the SMA hysteresis cycle. In these applications, the SMA converts the mechanical energy of structural oscillations into heat, which dissipates to the surroundings. However, effective

dampers built in the past, 20 years ago or more, showed several potential difficulties regarding SMA integration.[1]

In temperature and stress, hysteresis behavior appears, which includes intrinsic actions: between interphases and dislocations, with grain boundaries and precipitates. For induced stress, internal interactions contribute to the hysteresis width. The temperature actions produced by the absorbed and released latent heat, which locally modify the temperature, must also be considered. Moreover, the dissipated power in the sample, associated with the cycling rate and convective heat transfer, critically affects the sample temperature. The stress required for interface displacement therefore changes, which modifies the hysteresis width. Other particular actions can appear with changes in temperature or in stress aging. Aspects of strain aging are discussed below.

The particular requirements for the damping of stayed cables in bridges are somewhat more severe than those for the mitigation of earthquakes. The number of working cycles is much higher in strong storms (i.e., the northwesters of Western European coasts, typhoons, tropical cyclones, or hurricanes). For frequencies of several hertz, a strong storm lasting three or four days induces more than one million oscillations. The outside temperature conditions are also more rigorous. In earthquakes, dampers are typically situated inside the building, smoothing the daily and yearly temperature fluctuations. Meanwhile, on bridges, the dampers remain under the direct action of weather for year-long terms of use, at least. In Western Europe, the temperature change between summer and winter reaches the order of 40–50 K.

In general, "the barriers to the expanded use of SMAs include the high cost, lack of clear understanding of thermomechanical processing, dependency of properties on temperature, and difficulty in machining" [31]. The practical aim here focuses on the analysis of two examples of damping using SMA in realistic tests in facilities. The core of the analysis is the study of basic conditions to ensure appropriate and guaranteed behavior.

Increasing the quality of life is a major goal for smart materials and systems. In bridges, this takes the form of suppressing or reducing external perturbation phenomena by wind, rain, or traffic, which induce cable oscillations. Such oscillations induce progressive damage and failure of the steel fibers, with nonnegligible reductions in the cable life. In a classical effect, on the Dongting Lake Bridge over the Yang-Tse River, opened in 2002 [39], strong wind- and rainstorms induced greater oscillations for larger bridge cables. The bridge was retrofitted using magnetorheological (MR) dampers by LORD [40, 41].

Potential or practical damage was also observed in the cables of "old" French bridges. In FP014-SMARTeR: Shape Memory Alloys to Regulate Transient Responses in Civil Engineering (SMARTeR: 2006–09), one European Science Foundation (ESF) project investigated the application of SMAs for the damping of stayed cables [42]. In particular, it reported the problems appearing in the Iroise Bridge (constructed 1994) on the Élorn River near Brest with lower damage. Figure 1 shows the Saint-Nazaire Bridge (constructed in 1975) over the Loire River near Nantes. In this case, several cables were changed.

Oscillations can also appear under lower-velocity winds. Minor oscillations of $\sim$ 10 mm were observed under winds of speeds below 10 km/h in the larger 110-m cables of the Echinghen Viaduct (constructed 1997), situated on the A16 toll highway near Boulogne in the northwest region of France. The cables showed some damage; mitigating the oscillation amplitude could have increased the practical lifetime of the cables. Oscillatory damping requires the use of appropriate passive or semiactive dampers in the structure. Semiactive devices [1.2], as used in the LORD MR dampers in the Dongting Lake Bridge, require guaranteed electrical power and appropriate technical computing supervision, i.e., through both software and hardware management. Figure 2 shows an outline of partial free oscillations in the Dongting Lake Bridge.

Fig. 1 Saint-Nazaire Bridge over the Loire River near Nantes (West of France); three cables were changed

[1] The information available for the NiTi dampers established by the ISTECH project [37] and situated on the roof of the Basilica of San Francesco Assisi (in Assisi, Perugia, Italy) is poor. The ambient temperature effects on the SMA [38] seem irrelevant to the SMA behavior. On the ceramic roof of the Basilica, the temperature difference between sunny days in summer and cold days in winter probably exceeds 60–70 K. Using a value of 6.3 MPa/K for the CC thermodynamic equation, the global change in stress associated with a temperature change of 70 K approaches 450 MPa. The alloy can remain in the martensite phase in winter; in summer, the SMA remains austenitic without transformation. An easy crash can be expected by the increased stress and reduced fracture lifetime at higher stresses.

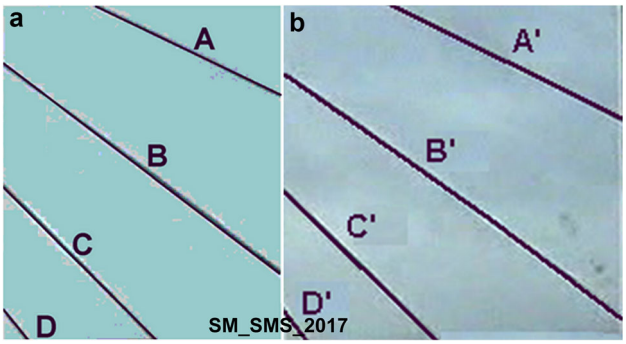

Fig. 2 Outline of the oscillations in the stayed cables of the Dongting Lake Bridge over the Yang-Tse River. The two images are separated by 0.53 s. The vertical displacement of cable B was close to 1 m. Built from data extracted from an old LORD video

Incorporating SMA wires as dampers in cables requires the appropriate fixation of the ends of the wires. Figure 3a, b, c shows the devices used, which avoid slippage of the SMA wires under forces exceeding 1 kN. These fastenings were realized by hardened steel cubes attached with four bolts. The device avoids the eventual bending of the wires induced by the compressive components of the oscillations by free displacement of cubes and SMA, as well as that induced by the eventual accumulated creep in the wires under repeated cycling.

This study of damping was performed in the two facilities of the European Laboratory for Structural Assessment (ELSA) at the Joint Research Center of the European Union, located in Ispra, Italy; and the Institut Français des Sciences et Technologies des Transports, de l'Aménagement et des Réseaux (IFSTTAR) in Bouguenais near Nantes. Figure 4 shows the cable equipment located outside the ELSA building (Fig. 4a) and the system used (Fig. 4b), in which cable A is one steel cable inside a polyethylene tube refilled by wax. B indicates the SMA wire and fixing device, and C is a rigid bar transmitting motion to the bottom with linear variable differential transformer (LVDT) position sensors.

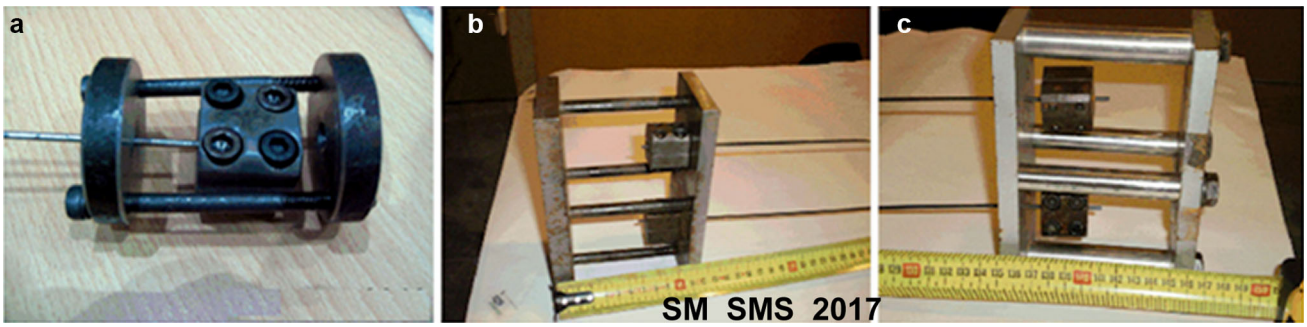

Fig. 3 Ends of the SMA wires in **a** ELSA and **b** and **c** IFSTTAR. The fastening device permits free slippage of the SMA wires under oscillations with compressive components

Fig. 4 **a** ELSA cables 1–2–3–4. **b** Connections. *A* Cable No 1. *B* SMA wire link. *C* "Rigid" bar transmitting the cable position to the LVDT situated in the bottom

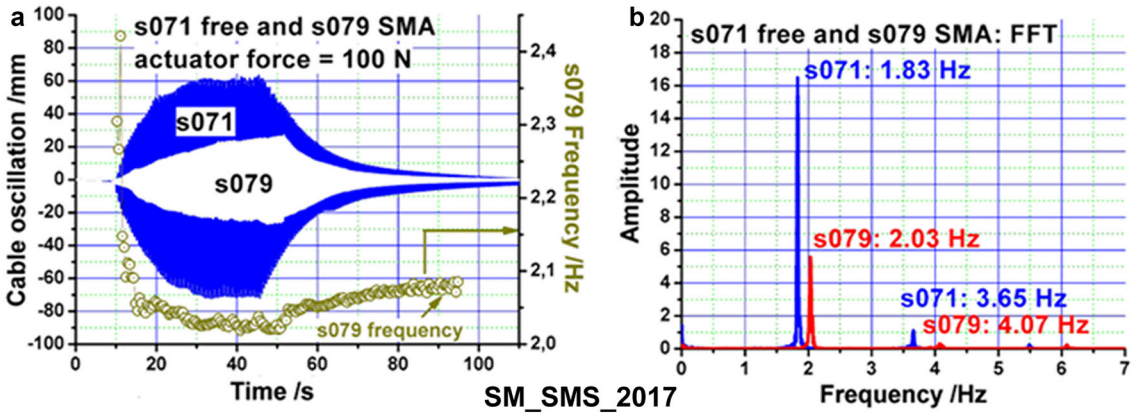

Fig. 5 ELSA results in steady oscillations under similar forces. **a** s071: Free oscillations. s079: SMA-damped oscillations by a trained SMA wire. Empty dots: frequency evolution in s079. **b** FFTs of s071 and s079

Figure 5 outlines the steady-state results. In Fig. 5a, the free cable oscillations at s071 and the SMA-damped oscillations at s079 with similar force action. Generally speaking, the oscillation amplitude is reduced by 3% and the associated energy is reduced to 10%. The progressive reduction of the amplitude modifies the force on the SMA according to the hysteretic behavior; the effect is a progressive change in frequency (see the s079 frequency). Figure 5b shows the fast Fourier transforms (FFTs) of s071 and s079; a minor increase in the mean frequency appears under the SMA load.

Two measurement campaigns were performed in IFSTTAR (Fig. 6) for the same 50-m steel cable (Fig. 6A). The second was realized during a relatively harsh winter (2010) with continuous low temperatures of − 2 to − 4 °C. A force sensor was used in the 2009 campaign (Fig. 6A, a). The SMA (B, b–b′) damper used two relatively short wires; the cable was pushed up and suddenly released. The transient cable oscillations were recorded using one laser (Fig. 6B, c).

Figure 7 shows the free oscillation of the cable with extremely low damping (Fig. 7a) and the effects associated with the SMA damper. Smoothing was moderately "reduced" in 2010, eventually related to the low temperature of the SMA. Transient signals in the free cable required some minutes to stop; with SMA, the signal disappeared in ∼ 10 s. The changes in the transformation working point in the SMA, with a change in the mean stiffness, induced a progressive increase of frequency in the oscillations. In Fig. 7, the "up" and "down" frequency values were calculated by FFT for the positive and negative parts of the signals, respectively. The SMA stiffness was associated with the maximal deformation observed in the hysteresis cycle and affected by the external temperature. The calculated frequency changes did not seem to have relevant effects.

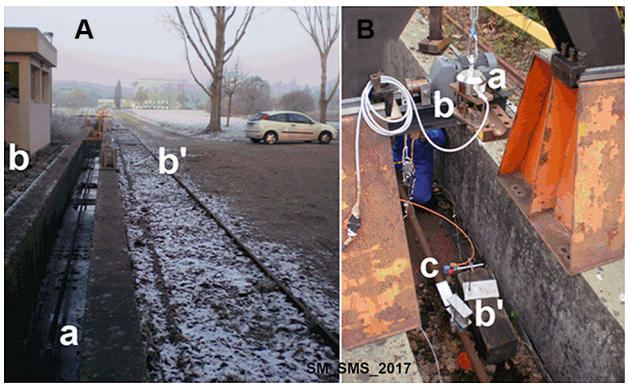

Fig. 6 The working space in IFSTTAR in the 2010 campaign with permanent ice in the fields. Measurements were performed on transient oscillations in a cold winter. **A** Cable allocation. *a* Cable. *b* and *b′* Rails for mobile equipment around the cable. **B** SMA wire dampers. *a* Force sensor. *b* and *b′* Ends of the two wire grips. *c* flat surface on the cable, permitting a mirror for the laser signal

Part Two: Specific Properties of NiTi SMA

The hysteretic behavior of NiTi wires was studied to optimize their applicability in dampers for civil engineering. The advantages of thick wires were clarified by this investigation. The study included the parasitic effects related to external hard winter temperatures. The specific properties of strain-aged wires are discussed.

Figures 8 and 9 show the progressive changes induced by 100 sinusoidal cycles with the maximal strain of 8% at 0.01 Hz. The working temperature in the laboratory was near 293 K. The thick wire (2.46 mm in diameter, shown in Figs. 8a and 9a) underwent severe deformation, with SMA creep of 2% and S-shaped cycles having a maximal stress near 600 MPa, similar to the maximal stress in the first cycle. The first cycle is the preliminary training used for the damper. The thinner wire (0.5 mm in diameter) with relevant SMA creep remained flat in cycle shape and the

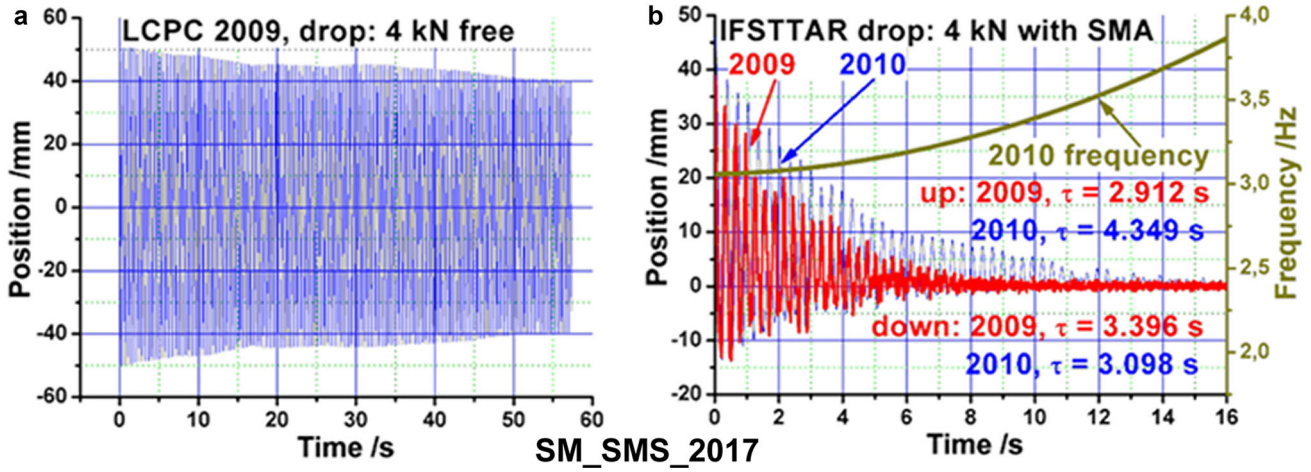

Fig. 7 IFSTTAR: 50-m cable. **a** Free oscillations in the middle of the cable. **b** Associated oscillations using two trained SMA wires in 2009 and 2010 measurement campaigns

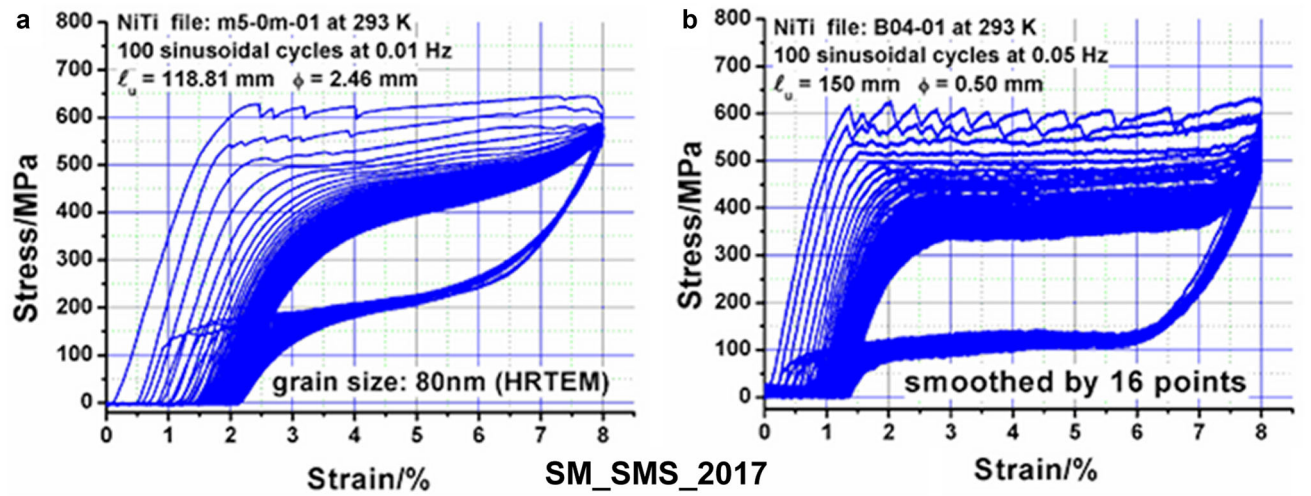

Fig. 8 100 sinusoidal cycles with a maximal strain of 8% at 100 and 20 s in **a** thicker and **b** thinner wires

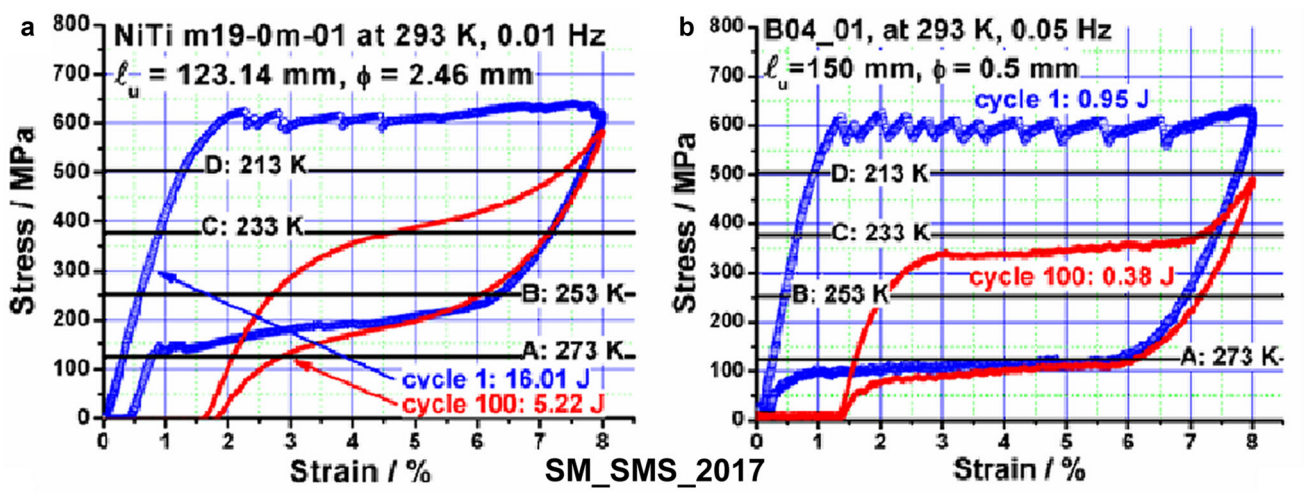

Fig. 9 Cycle 1 and cycle 100 for **a** thick and **b** thinner wires. The first cycle shows nucleation effects. **a** Sample of 2.46 mm. **b** Sample of 0.5 mm. Continuous lines show preliminary effects on the "base line" for winters at *A* 273 (i.e., 0 °C), *B* 253, *C* 233, and *D* 213 K

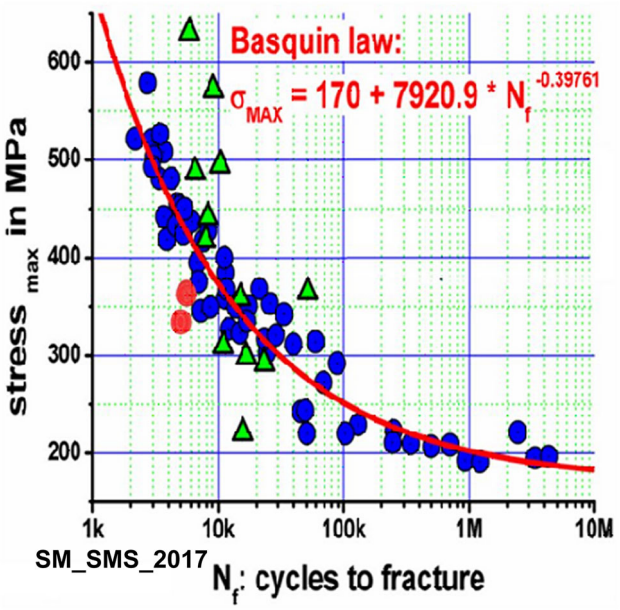

Fig. 10 Several sets of samples in stress against number of cycles before fracture for NiTi wire of 2.46 mm in diameter

retransformation occurred near 100 MPa. In thinner wires, training was faster (i.e., 0.05 Hz) according to the ratio between the diameters, i.e., 0.05 Hz for the 0.5-mm diameter. In a cylindrical wire, avoiding the internal effects, elementary heat transfer was proportional to the radius. A similar transmission required simultaneous scaling in both radius and time (1/frequency).

Figure 9 outlines the expected effects of the external temperature for the NiTi wire with a Clausius–Clapeyron coefficient of 6.3 MPa/K. Reducing the room temperature, i.e., to 273, 253, … K, relocates the base line at progressively increasing levels. The measurements indicate that the thin wire cannot retransform at 273 K (0 °C), but that the thick wire experiences minor hysteretic cycles at temperatures as low as 253 K (− 20 °C).

The application of SMA wires requires an appropriate fracture-life for the wires. In general, the number of oscillations is associated with the expected number of storms and the oscillating frequencies. For storms lasting 3 or 4 days and the basic frequency of 1 Hz, the required number of cycles exceeds 0.5 million. Figure 10 contains several series of measurements between 600 and 200 MPa with reduced strains at lower stresses. Globally, the experimental points are fitted by Basquin's law. In this case, the exponent probably associated with MT is clearly different from the classical values associated with the elastic part.

Figure 11 outlines the effects of different external temperatures on multiple consecutive cycles. In A-top, the evolution of the energy against the temperature is shown. In B-bottom, the continuous cycles are shown against temperature. The cycles in points A, B, C, D, and E and the corresponding temperatures are shown in Fig. 11b.

Self-Heating

Cycling induces thermal effects related to partial or complete cycles by the heat dissipated and absorbed in the transformation–retransformation processes. Slow cycling at 0.01 Hz and the strain of 8% produces temperatures higher and lower than room temperature (Fig. 12a). A progressive increase in frequency (Fig. 12b) induces relevant self-heating (near 25 K for strains of 8% and cycling at 3 Hz). Faster low-strain cycling (i.e., 1 and 0.8%) also produces relevant self-heating (Fig. 12c).

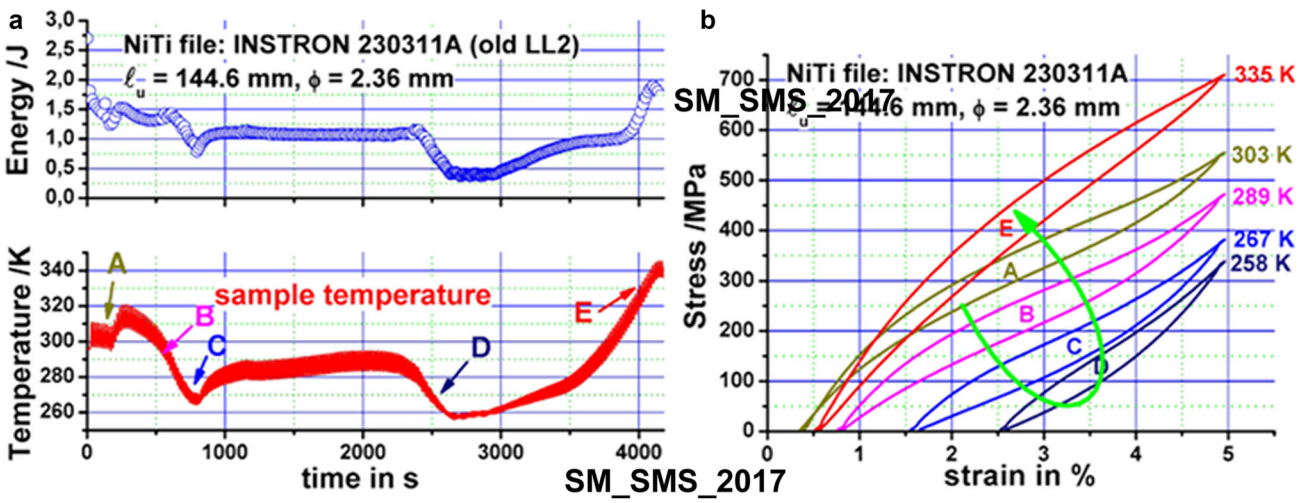

Fig. 11 Thick (S-shaped) effects in the hysteresis cycle under summer–winter external temperature changes. **a** Dissipated energy against time (maximal strain ∼ 5%). **b** Hysteresis cycle and associated temperatures

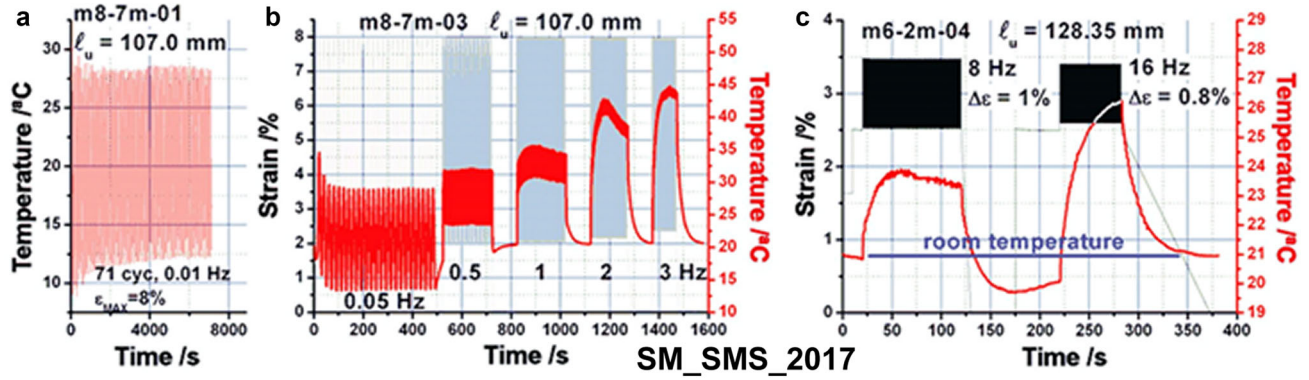

Fig. 12 The sample temperature changes associated with cycling rate in NiTi wire of 2.46 mm in diameter. **a** Cycling at 0.01 Hz with 8% of maximal deformation. **b** From 0.05 to 3 Hz, the self-heating passes from one temperature wave (tracking the strain) to one dissipative phenomenon. **c** Faster cycling at low strains (1 and 0.8%)

Strain Aging at 373 K

The S-shaped wire with a maximal stress of about 600 MPa permits appropriate work in moderate winters as, for instance, with temperatures of 263–253 K. The interest of an improved strain aging focuses on the increased stress, i.e., up to 900–1000 MPa. The high stress permits satisfactory working in cool winters (i.e., 243–233 K). In their actual state of the art, the strain aging requires deep study analyzing the different behaviors, which shows the thick and the thin wires and their associate fatigue/fracture effects. The effects that appeared in the thinner wires are described below.

The analysis was carried out using thick and thin wires of 2.46 and 0.5 mm in diameter, respectively. The samples of nearly 180 mm in length were housed in a strain-aging device (Fig. 13a) that, after aging, could be placed in a traction machine without mounting or dismounting processes during continuous analysis (Fig. 13b). The possibility of cycling without the need for dismounting of the sample-holding device avoided undesirable changes in the sample length. When the device was housed in the MTS (hydraulic stress–strain equipment), the previous strain was relaxed, with the measurements starting with zero stress. The cubes A and A′ held the sample in position. The screw B and bolt D are used to modify the length of the sample. After completion of strain aging, the device was placed in a furnace at 373 K for several days or months.

Using the as-furnished samples, the strain aging induced an increase in the maximal stress related to the time elapsed in aging. Later, the training of the strained samples reduced the width of hysteresis, as shown in Fig. 14. Using the as-furnished samples thus seems improper. Figure 15 outlines the differences between the "as-is" sample behaviors for different strain-aging programs (Fig. 15a, b) and the previously trained samples, as shown in Fig. 15c. The conventional storing of samples at room temperature

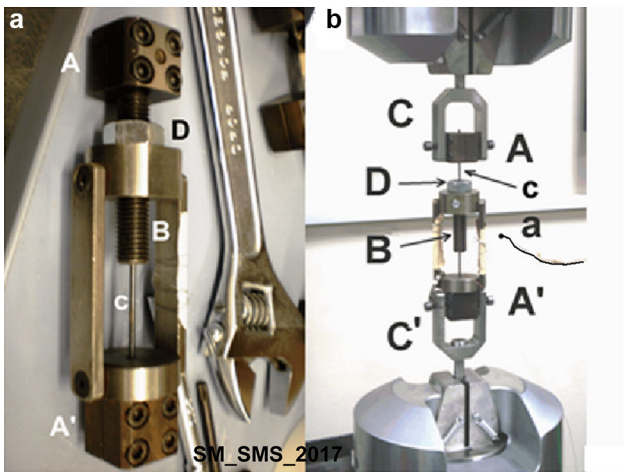

Fig. 13 **a** Adapted device for stress–temperature aging. *A*, *A′*: Cubes that fasten the ends of the sample c. *B* and *D*: screw and the associated bolt that enable modification of the sample length by applied stress. **b** Stress-aging device and cycling in the MTS without dismounting of the sample. *C* and *C′*: Auxiliary grips avoiding compression and permitting slippage of the sample, induced by SMA creep. a: Room-temperature thermocouple

seems to have no relevant effects. One year of room-temperature storage does not change the strain-aging effects (Fig. 15c). Some structural effects were probably induced by the strain aging at 373 K. The results require further analysis.

Strain Aging in Thinner Wires

The standard cycling, i.e., training by 100 cycles at 8%, produces different behaviors for thick and thin wires, as shown in Fig. 9. The actions of strain aging also differ between wires of the two diameters, suggesting some intrinsic differences between the internal crystallographic structures of the wires. Figure 16 outlines the strain-aging

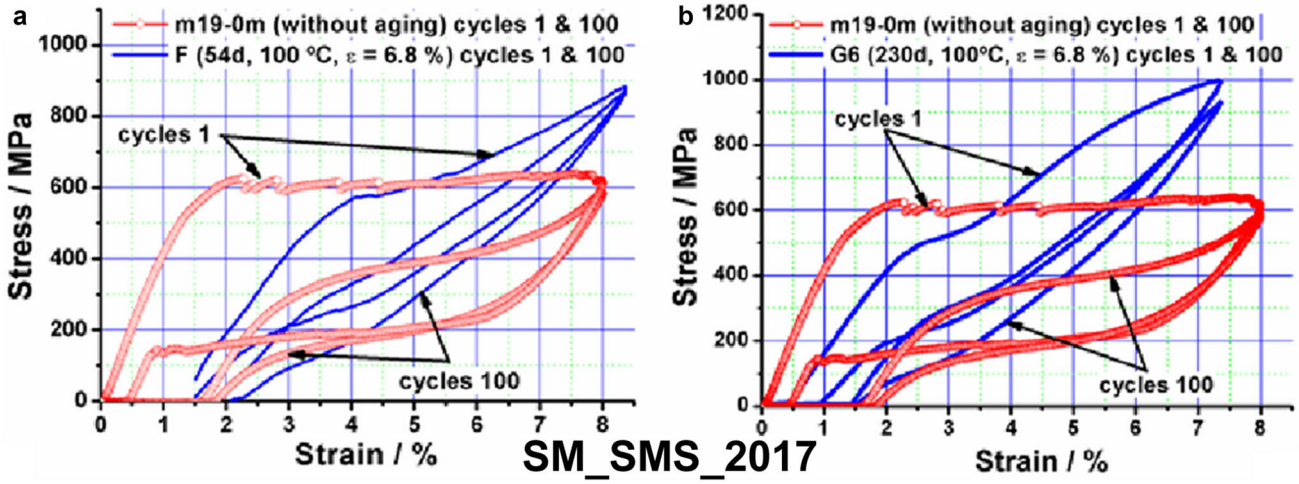

Fig. 14 Results for stress aging at 373 K for a wire of 2.46 mm in diameter. Empty dots: Data from the as-furnished wire. Line: Data from the strain-aged sample. **a** About 2 months' aging for a strain of 6.8%; **b** 7 months' aging for a strain of 6.8%

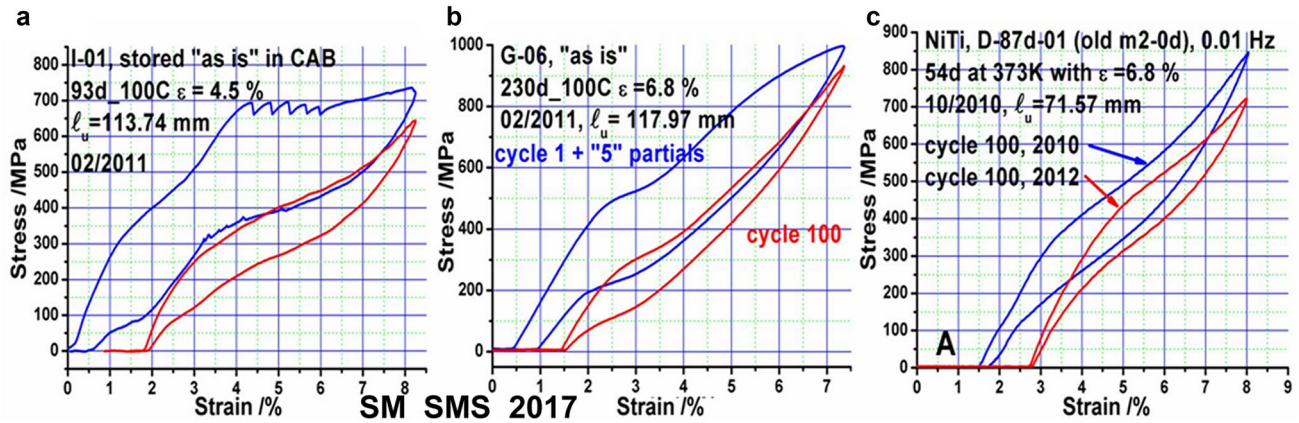

Fig. 15 **a** Moderate strain (4.5% for 93 days) applied to the as-furnished sample. **b** Strain of 6.8% applied for 230 days to the as-furnished sample. **c** Permanent effects appearing in a previously cycled sample using a strain of 6.8% for 54 days (year 2010). Minor changes are observed after 1 year at room temperature (year 2012)

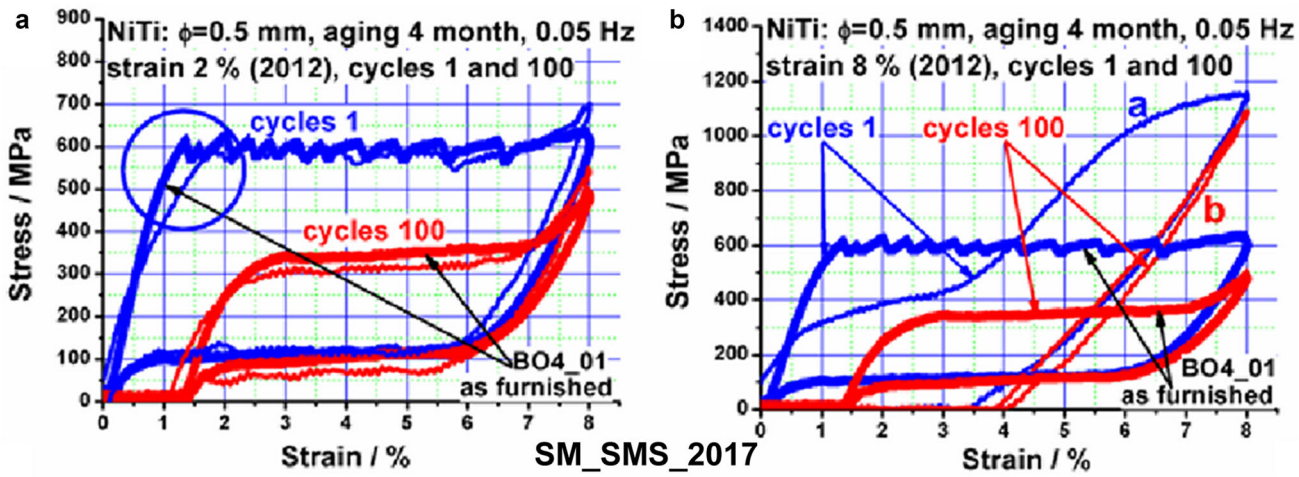

Fig. 16 Two examples of strain-aging results for wires of 0.5 mm in diameter. **a** About 4 months' aging at 2% deformation inducing reduced action (circle in **a**) and similar nucleation effects. After training, this effect has completely disappeared. **b** The more significant effect for a larger strain (8%) for 4 months at 373 K

effects in the wire of 0.5 mm in diameter. Four months of reduced strain (2%) produced no particular change after training (i.e., Fig. 16a). Using one strain of 8% for 4 months, a maximal stress of 1000 MPa and an extremely reduced hysteresis appeared (i.e., Fig. 16b). This experimental result suggests that, in this case, the sample is practically converted to the martensite phase. The previously stressed sample is enlarged with a reduction of the initial stresses induced by the strain device. In other words, after aging, the initial stress almost disappears. Cycle 1a shows the classical behavior associated with the reorientation of martensite in the direction of the applied stress. Cycle 100b, with an initial SMA creep of 4%, is practically elastic in nature, with no hysteresis. An increase in the ambient temperature using the furnace system in the INSTRON machine returned the alloy to the parent phase under standard cycling.

Conclusions

The experimental analysis of SMA NiTi wires, including results from studies within facilities, shows their capabilities in the damping of stayed cables for steady and transient signals.

The study of the wires suggests that thicker wires have distinct advantages over thinner wires. The partial training of thick wires induced an S-shaped behavior that permitted external temperatures as low as − 20 and − 30 °C. However, the thinner wires showed reduced retransformation stresses if they retained flat cycles (for instance, with actuators). At low temperatures, the thinner wires could not retransform and cannot be considered useful.

Preliminary studies on the strain aging of thick wires showed increased maximal stresses reaching 900–1000 MPa, which permitted appropriate work in extremely cold winter temperatures reaching between − 40 and − 60 °C. The strain aging results suggested that different behaviors occurred in the thick versus thin wires. The thinner wires seemed to transform completely to martensite. This suggests that scaling of SMA wires between different applications must be performed carefully in facilities with experimental controls to ensure satisfactory behavior.

Acknowledgements Technical supports from the Materials Laboratory of the Atomic Center of Bariloche, 8400 Argentina; of the facilities in stayed cables of ELSA, Ispra, Italy; and the cable studies of IFSTTAR, Bouguenais, France, are gratefully acknowledged.

References

1. Ehrenfest P (1933) Phase changes in the ordinary and extended sense classified according to the corresponding singularities of the thermodynamic potential. Proc Acad Sci Amsterdam 36:153–157
2. Landau LD (1937) Zur Theorie der phasenumwandlungen II. Phys Z Sowjetunion 11:26–35
3. Lovey FC, Torra V (1999) Shape memory in Cu-based alloys: phenomenological behavior at the mesoscale level and interaction of martensitic transformation with structural defects in Cu-Zn-Al. Prog Mater Sci 44–3:189–289
4. Torra V, Isalgue A, Lovey FC, Sade M (2015) Shape memory alloys as an effective tool to damp oscillations. Study of the fundamental parameters required to guarantee technological applications. J Therm Anal Cal 119(3):1475–1533
5. Torra V, Auguet C, Isalgue A, Carreras G, Lovey FC (2013) Metastable effects on martensitic transformation in SMA Part IX. Static aging for morphing by temperature and stress. J Therm Anal Calorim 112:777–780
6. Torra V, Carreras G, Lovey FC (2015) Effects of strain aging at 373 K in wires of NiTi shape memory alloy. Can Metall Q 54–1:77–84
7. Torra V, Auguet C, Isalgue A, Carreras G, Terriault P, Lovey FC (2013) Built in dampers for stayed cables in bridges via SMA. The SMARTeR-ESF project: a mesoscopic and macroscopic experimental analysis with numerical simulations. Eng Struct 49:43–57
8. Torra V, Carreras G, Casciati S, Terriault P (2014) On the NiTi wires in dampers for stayed cables. Smart Struct Syst 13–3:353–374
9. Isalgue A, Torra V, Yawny A, Lovey FC (2008) Metastable effects on martensitic transformation in SMA Part VI. The Clausius-Clapeyron relationship. J Therm Anal Calorim 91(3):991–998
10. Torra V, Carreras G, Casciati S, Terriault P (2014) On the NiTi wires in dampers for stayed cables. Smart Struct Syst 13(3):353–374
11. Otsuka K, Wayman CM (eds) (1998) Shape memory materials. Cambridge University Press, Cambridge
12. Wayman CM (1992) Shape memory and related phenomena. Prog Mater Sci 36:203–224
13. Otsuka K, Ren X (2005) Physical metallurgy of Ti-Ni-based shape memory alloys. Prog Mater Sci 50(5):511–678
14. Mohammad HE, Mandi H, Majid T, Bhaduri SB (2012) Manufacturing and processing of NiTi implants: a review. Prog Mater Sci 57(5):911–946
15. Ishida A, Sato M, Takei A, Miyazaki S (1995) Effect of heat treatment on shape memory behavior of Ti-rich Ti-Ni thin films. Mater Trans, JIM 36(11):1349–1355
16. Kim JI, Kim HY, Hosoda H, Miyazaki S, Satoru H (2004) Mechanical properties and shape memory behavior of Ti-Nb alloys. Mater Trans, JIM 45(7):2443–2448
17. Kim JI, Kim HY, Hosoda H, Miyazaki S (2005) Shape memory behavior of Ti–22Nb–(0.5–2.0)O (at%) biomedical alloys. Mater Trans, JIM 46(4):852–857
18. Kanetaka H, Hosoda H, Shimizu Y, Kudo T, Zhang Y, Kano M, Sano Y, Miyazaki S (2010) In vitro biocompatibility of Ni-Free Ti-based shape memory alloys for biomedical applications. Mater Trans, JIM 51(10):1944–1950
19. Janocha H (ed) (1999) Adaptronics and smart structures. Springer, Berlin
20. Kohl M (2004) Microactuators. Springer, Berlin
21. Van Humbeeck J (1999) Non-medical applications of shape memory alloys. Mat Sci Eng A 273–275:134–148

22. Mekki OB, Auricchio F (2011) Performance evaluation of shape-memory-alloy superelastic behavior to control a stay cable in cable-stayed bridges. Int J Non-Linear Mech 46(2):470–477
23. Torra V, Isalgue A, Auguet C, Carreras G, Lovey FC, Terriault P, Dieng L (2011) SMA in mitigation of extreme loads in civil engineering: damping actions in stayed cables. Appl Mech Mater 82:539–544
24. Sharabash AM, Andrawes BO (2009) Application of shape-memory alloy dampers in the seismic control of cable-stayed bridges. Eng Struct 31(2):607–616
25. Casciati S, Faravelli L (2008) Structural components in shape-memory alloy for localized energy dissipation. Comput Struct 86:330–339
26. Zhang Y, Zhu S (2008) Seismic response control of building structures with superelastic shape-memory alloy wire dampers. J Eng Mech 134(3):240–251
27. Alam MS, Youssef MA, Nehdi M (2007) Utilizing shape-memory alloys to enhance the performance and safety of civil infrastructure: a review. Can J Civ Eng 34(9):1075–1086
28. Yawny A, Sade M, Eggeler G (2005) Pseudoelastic cycling of ultra-fine-grained NiTi shape-memory wires. Zeitschrift für Metallkunde 96(6):608–618
29. Torra V, Isalgue A, Martorell F, Terriault P, Lovey FC (2007) Built in dampers for family homes via SMA: an ANSYS computation scheme based on the mesoscopic and the microscopic experimental analysis. Eng Struct 29:1889–1902
30. Auguet C, Isalgué A, Lovey FC, Martorell F, Torra V (2007) Metastable effects on martensitic transformation in SMA Part 4. Thermomechanical properties of CuAlBe and NiTi observations for dampers in family houses. J Therm Anal Calorim 88(2):537–548
31. DesRoches R, Smith B (2004) Shape memory alloys in seismic resistant design and retrofit: a critical review of their potential and limitations. J Earthq Eng 8(3):415–429
32. Dolce M, Cardone D (2001) Mechanical behaviour of shape memory alloys for seismic applications 2. Austenite NiTi wires subjected to tension. Int J Mech Sci 43:2657–2677
33. Dolce M, Cardone D (2001) Mechanical behaviour of shape memory alloys for seismic applications 1. Martensite and austenite NiTi bars subjected to torsion. Int J Mech Sci 43:2631–2656
34. Wollants P, Debonte M, Roos JR (1979) A thermodynamic analysis of the stress induced martensitic transformation in a single crystal. Z Metallkunde 70:113
35. Wollants P, Roos JR, Delaey L (1993) Thermally- and stress-induced thermoelastic martensitic transformations in the reference frame of equilibrium thermodynamics. Prog Mater Sci 37(3):227–288
36. Wollants P, Roos J, Otsuka K (1991) On the thermodynamic-equilibrium of stress-induced martensitic transformations. Zeitschrift fur metallkunde 82(3):182–185
37. Project ENV4-CT95-0106. http://ec.europa.eu/research/press/2001/pr0510en.html
38. Indirli M, Castellano MG (2008) Shape memory alloy devices for the structural improvement of masonry heritage structures. Int J Archit Herit 2(2):93–119
39. http://en.wikipedia.org/wiki/Dongting_Lake_Bridge
40. http://www.lord.com/Products-and-Solutions/Magneto-Rheological-(MR).xml
41. Chen ZQ, Wang X Y, Ko JM, Ni YQ, Spencer BF Jr., Yang G (2003) MR damping system on Dongting Lake cable-stayed bridge. Smart structures and materials 2003: smart systems and nondestructive evaluation for civil infrastructures. In: Liu S-C (ed) Proceedings of the SPIE, vol 5057, pp 229–235. https://doi.org/10.1117/12.498072
42. http://www.esf.org/activities/eurocores/completed-programmes/s3t/projects.html